

Compressibility curves of iron-base powders: Support for evaluating stresses on compaction tools or just a method for evaluation of raw materials?

© 2018 G.F. Bocchini, Italy

Received 17.05.18, accepted for publication 22.05.18

The forecast of maximum stresses on compaction tools is frequently based on the so-called compressibility curves, obtained according to specific standards. The analysis of compressibility curves enables to draw a simple analytical law, to utilize for further developments. The relationship between radial and axial pressure is described. The radial pressure is the design datum for the correct dimensioning of dies. Literature data on the relationship between applied pressure and friction coefficient enables to derive a model linking compact geometry and axial pressures effectively needed to reach specific densities. For part shapes characterized by a discrete extension on height – such as bushings, for instance – the effects of geometry are linked to 2 dimensionless parameters, one of physical nature (product of the pressure ratio multiplied by friction coefficient) and one of geometrical nature (ratio between «vertical» friction surfaces and double of compaction area). These dimensionless parameters enable to draw the «real» compressibility curves, linked to specific geometries. For part shapes characterized by small height – such as thin disks or plates – the effects of geometry again depend on two dimensionless parameters: one of physical nature (ratio between two times the friction coefficient and pressure ratio) and one of geometrical nature (ratio radius/height of the thin disk). Thinner the disk, higher the pressure needed to attain a given density. The theoretical results are compared with experimental data. The agreement between experimental data and forecasts based on the theoretical approach is good. The study proves that the standard compressibility curves, if uncritically utilized for predicting stresses acting on tools, are unsuitable to predict the stresses really acting at compaction end.

Keywords: compressibility, density, P/M tooling & design, tribology.

Bocchini Gian Filippo – Dr., P/M consultant, Rapallo (Genova), Italy. E-mail: bocchini.mp@libero.it.

Citation: Bocchini G.F. Compressibility curves of iron-base powders: support for evaluating stresses on compaction tools or just a method for evaluation of raw materials? *Izv. vuzov. Poroshk. metallurgiya i funkts. pokrytiya*. 2018. No. 4. P. 32–47. DOI: dx.doi.org/10.17073/1997-308X-2018-4-32-47.

Introduction

Every mechanical part to be used with safety must have a strength, — static and fatigue — appropriately higher than the load expected on operation. Furthermore, in the case of parts characterized by functional requirements of fair or good accuracy, the acting stresses must be lower than the stresses capable of causing plastic yielding of the provided material. In the case of P/M iron-based materials, peculiarly porous, with porosity ranging generally from 16 to 5 %, the mechanical strength, static or dynamic, is a function of density, type of alloying, sintering conditions, possible heat treatment, including sinter-hardening. As to the influence of density, the data in the literature are numerous, but not completely univocal. Presumably, in the USA, A. Squire, [1], was the first scientist to publish experimental results, as shown by Fig. 1. That chart became almost a classic, because P.W. Lee, [2], F.V. Lenel, [3], and, after half a century, J. Kosko, [4], republished the

same plot. Even R. Kieffer and W. Hotop, [5] published the Squire's results, with the additional indication that the American scholar had also studied the shear strength of sintered iron and had found an exponential law of dependence on density. A couple of years after A. Squire, also M.Ju. Balschin, in Soviet Union, [6], found experimentally a law of dependence of the same type, then confirmed in his text [7]. Always in past times, W.V. Knopp, [8], and G.S. Pisarenko, V.I. Troshchenko and A.Ya. Kravsovskii [9] arrived at similar results. A few years later, H.H. Hausner, [10], published graphs, for P/M steels (7 % Ni, from 0 to 0.8 % C, density between 6.4 and 7.6 g/cm³), which clearly show exponential trends. The first contradictions appear with F.V. Lenel, [3], which published three graphs, relating to steels of different composition, with conflicting trends: exponential, parabolic, linear. F.V. Lenel states that the data came from an ASM publication, [11]. R.M. German, [12], proposes

once again an exponential type relation, with different slopes for different materials, as shown in Fig. 2, with both logarithmic scales. Surprisingly, R.M. German specifies that, in the first approximation, the correspondence between tensile strength and density should be linear, according to R.T. DeHoff and J.P. Gillard [13]. This hypothesis, however, is inconsistent with any fractographic observation, clearly indicating that the size of inter-particle necks, (certainly lower, in relative terms, of the fraction of observable metal area at LOM), limits the mechanical strength. R.M. German, however, in a subsequent text, [14], published a table on the relationship between UTS and density of a simple carbon steel (0.5 %), which clearly indicates a linear law. F. Thümmeler and R. Oberacker, [15], republished a graph initially made by G. Zapf, Fig. 3, [16], and specify: «In practice, the tensile strength can be often interpolated linearly for densities ranging from 6.5 to 7.5 g/cm³, while *rupture elongation* and *impact strength* present a stronger dependence on porosity. This is true for a number of sintered steels, while others show a rather different behavior of

the strength, with slope increase at high density... The linear dependence of strength from porosity, however, is not theoretically founded». Even W. Schatt and K.P. Wieters, [17], publish a diagram, due to G. Zapf, on which, for Cu-based sintered materials, the band of values clearly follows an exponential trend. P. Beiss, [18, 19], who published over 100 plots, is certainly the scien-

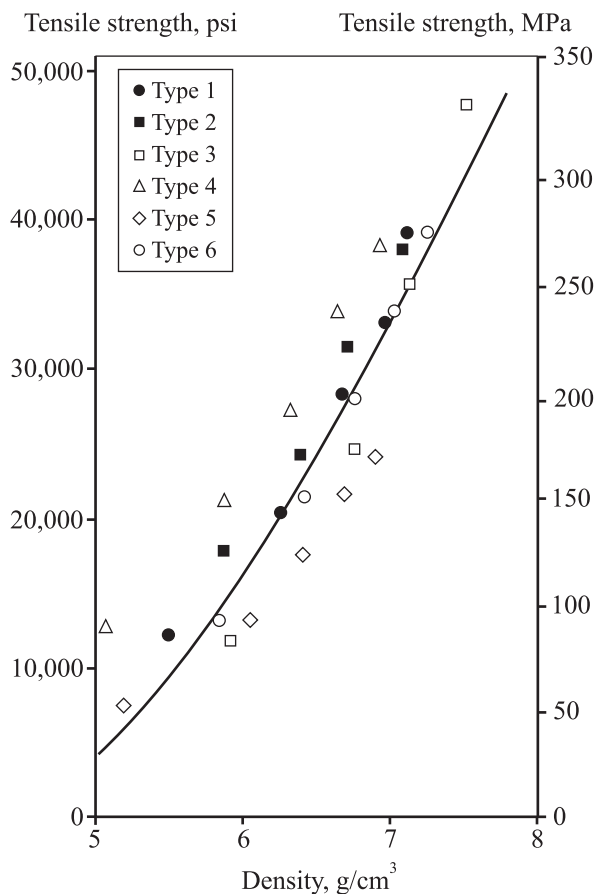


Fig. 1. Tensile strength versus density of sintered iron, from 6 powder grades; sint. one hour at 1100 °C (from F.V. Lenel [3])

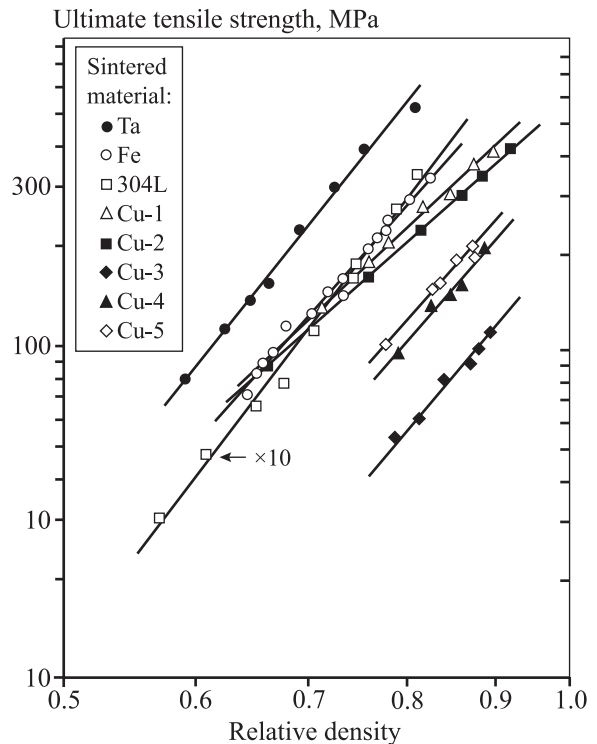


Fig. 2. Relationship between tensile strength and relative density of sintered materials (from R.M. German [12])

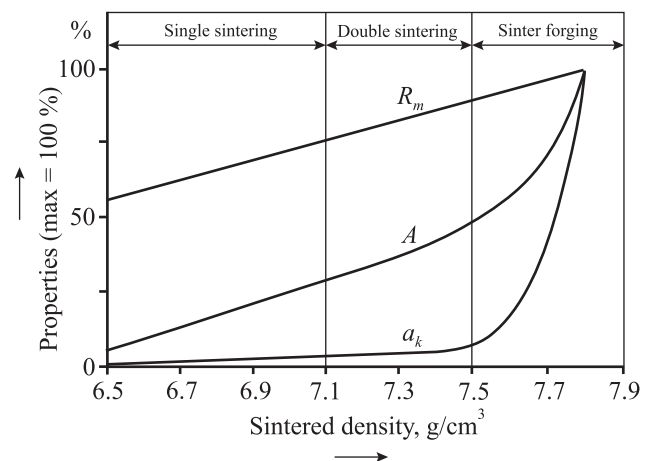


Fig. 3. Dependence of mechanical properties of P/M steels from sintered density (from G. Zapf [16])

R_m – ultimate tensile strength; A – rupt. elongation; a_k – fracture toughness

tist to be acknowledged as to quantity of data and graphs presented, where exponential trends prevail. As shown, the indications in the literature agree on one obvious fact: the mechanical strength of sintered materials is an increasing function of the density. The dependence law, however, does not appear univocal with certainty. Even the use of MPIF Standards, [20], or publications of very large powder producers, [21], does not allow drawing conclusive opinions. For completeness, we can stress that several authors attempted to model the mechanical behavior of porous materials, by means of different formulas, mainly of exponential type. Among the various proposed laws, the ones that seem to best match the experimental results are due to M. Eudier, [22], supplemented by G.F. Bocchini, [23], with the insertion of a pore form factor, and to H.E. Exner and D. Pohl, [24].

Determination of compressibility according to the Standards

As shown, the mechanical properties of sintered metallic materials depend on density. Furthermore, frequent requirements of good dimensional accuracy oblige to choose materials that exhibit small dimensional changes on sintering and, consequently, small density changes. Then, the ability to reach high densities on cold (or «warm») compaction defines the suitability of any iron powder to densification by application of pressure. The so-called compressibility curves graphically represent the density changes that occur when a metal powder (or a mix) is under pressure within rigid tools. National and/or international standards, [25–27], completely specify the test procedures. Fig. 4 shows a typical tool for compressibility test. Since the purpose of the test is to evaluate the behavior of metal powders under relatively high pressures, the portion of the curve that gives densities below 200 MPa is usually neglected. This implies that the compressibility curves are not usable when some transfer of powder mass is needed, to prepare the correct filling configuration before the beginning of pressure increase. Usually, the maximum test pressure is at least 700 MPa. The scales of the diagram are linear and pressure is plotted on the x -axis, while density is plotted on the y -axis. With only a few exceptions, the compressibility curves of metal powders are typical, with a pronounced convexity upwards.

The main reasons that lead to this trend are:

- the progressive decrease in the voids between particles, both as fraction and size;
- the work-hardening of the metal.

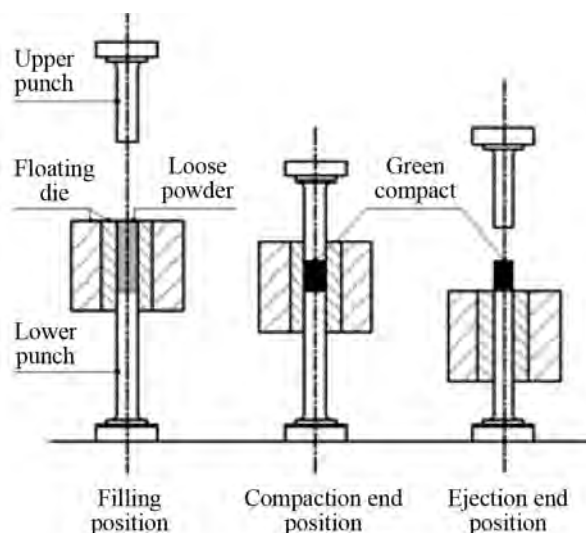


Fig. 4. Example of simple tool for compressibility test

By means of the compressibility curves we can measure an «absolute» property of a given powder (or powder mix), i.e. the law of density increases as a function of the applied pressure, according to a standardized procedure on reference samples. This method appears suitable to test and compare different metal powders, and mixtures thereof. However, at least a priori, it could be unsuitable to predict the behavior of a powder subjected to pressure, when the shape of the green part substantially differs from that of compressibility samples (small cylinders or parallelepipeds).

Analysis of friction conditions on different surfaces

In powder pressing the friction that contrasts densification acts between:

- a) powder and surfaces of die and core-rods;
- b) powder and faces of punches that apply pressure;
- c) surfaces of powder particles in contact and in relative motion.

The conditions of the tribological couples are substantially different, as shown, qualitatively, in Table 1.

If we consider the average specific surfaces of iron powders commonly utilized for manufacturing P/M parts, with some approximation, we can estimate that, in a 70 g compact, the total powder surface is $6.5 \cdot 10^4 \text{ cm}^2$, while other parameters change, as density increases, as shown in Table 2.

Even considering that the «true» surface of contact and sliding is a small fraction of the apparent, one, it should be clear that its value is still considerably high-

Table 1. Distinctive features of tribological couples on compaction

Contact zone	Die/powder	Punch/powder	Powder/powder
Case	<i>A</i>	<i>B</i>	<i>C</i>
Deformability of materials	Very different	Very different	Identical or very similar
Hardness of materials	Very different	Very different	Identical or very similar
Chemical affinity between materials	Modest	Modest	Very high
Extent of sliding	From very high to nothing	Very modest	From very high to modest

er than that of powder-tool contact surfaces, which, at 7.0 g/cm³ density, for compressibility test specimens, indicatively, are 10 cm² between punches.

Distinctive features of tribological couples on compaction and powder and 16 cm² between die and powder. These approximate evaluations show the basic role of lubricant for decreasing the resistance to densification coming from mutual sliding between powder particles. The importance sometimes given to wall lubrication seems worthy of a proper critical review.

Table 2. Features of pores and contact areas at two compaction densities; iron powder

Compact density, g/cm ³	5.0	7.0
Average pore volume, cm ³	3.03·10 ⁻¹⁰	1.30·10 ⁻¹⁰
Average pore diameter, cm	8.3·10 ⁻⁴	6.3·10 ⁻⁴
Total number of pores	1.54·10 ⁹	1.54·10 ⁹
Average pore surface, cm ²	2.16·10 ⁻⁶	1.25·10 ⁻⁶
Total pore surface, cm ²	33·10 ²	19·10 ²
Maximum inter-particle contact area, cm ²	6.17·10 ⁴	6.31·10 ⁴

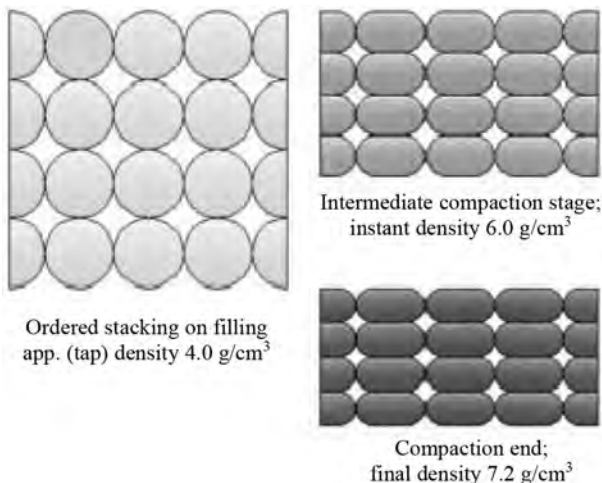


Fig. 5. Equally sized spherical particles arranged as fcc lattice: steps of plastic deformation on compaction

Since on compaction the pressure acts uniaxially, the plastic deformation of the particles is not isotropic. If we imagine the compaction of equally sized spherical particles, neatly stacked according to the fcc lattice, Fig. 5 shows, schematically, the ideal sequence of particle deformation. Actually, the particle shape is necessarily different from the spherical one (to ensure a sufficient green strength of compacts), while their size ranges within a broad spectrum, typically between about 0.02 and 0.18 mm.

Fig. 6, from W.B. James, [28], shows a section of a Fe + 2 % Cu pressed material, compacted according a vertical axis, after lubricant removal by suitable thermal process. Since the resistance to plastic deformation of copper particles is lower than that of iron particles, the harder granules squeeze the softer ones. In other words, the elongated shape of copper particles, predominantly on a nearly horizontal axis, appears as a clear sign of the anisotropy of plastic deformation in compaction.

Finally, Fig. 7 represents a schematic sequence, closer to real situations, also showing some movements of rotation (or rearrangement), imposed by the rigid punch face, which applies pressure, before the stage of material's plastic deformation begins.

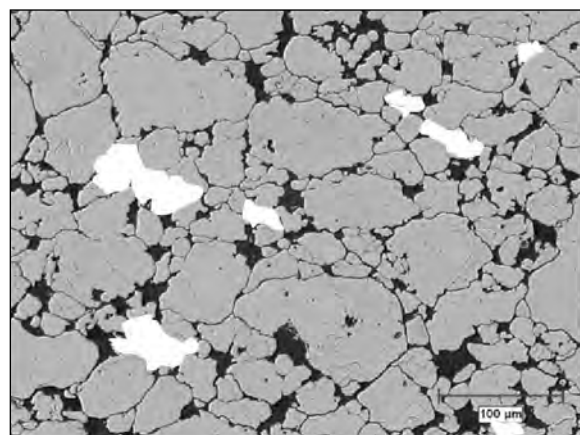


Fig. 6. Vertical cross-section (compaction axis) of a presintered compact; Fe + 2 % Cu (white section of particles) mix; atomized powder (from W.B. James [28])

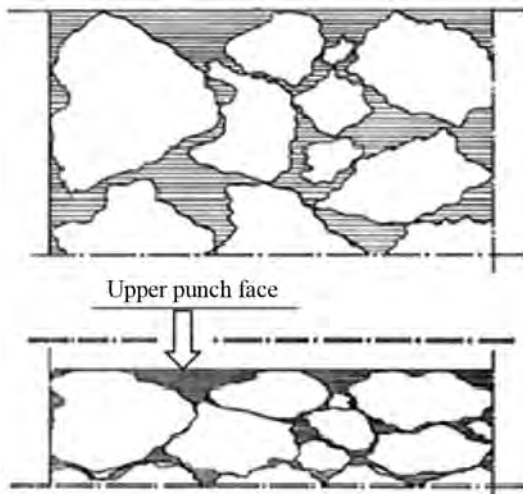


Fig. 7. Schematic representation of particle rearrangement, rotation and deformation, under the action of a rigid punch

Friction on the walls of die and core rods

A. Duffield and P. Grootenhuis, [29], have been the first scientists to analyze the equilibrium conditions of a thin powder layer, ideally isolated within a body subjected to axial pressure, and derived the formula that describes the variation of the axial pressure due to friction on the die walls, as a function of the distance from the faces of punches. They used a very simplified theoretical model, which, strictly speaking, may be valid only as a first approximation. In fact, in the analytic development, they assumed a plane stress state also for quite large surfaces. Referring to Fig. 8 and using suitable measurement units, let us indicate with:

A the compaction surface, u the contact perimeter between powder and die, (and core rods, if present),

p_i the uniform pressure applied at the instant t from both the upper and the lower punch (hypothesis of bilateral, symmetrical and simultaneous compaction), p the uniform pressure acting in axial direction, at the instant t , on a flat surface located at a certain distance, x , from the nearest punch, dh the infinitesimal thickness of a powder layer, (dh is measured as positive in the direction of increasing x), dp the small decrement of axial pressure on the infinitesimal thickness dx , consequence of the friction on the die (or lateral walls), originated by the radial pressure, p_r the radial pressure originated by the axial one, and to it proportional, μ the ratio between radial pressure and axial pressure, at t instant, H_i the height «snapshot» of the compact at t instant, p_n the minimum axial pressure, which acts at time t . Considering the ideal condition of perfect symmetry, the minimum pressure is that one acting at half height of the compact, on the mid-plane, in the so-called «neutral» zone, f the friction coefficient, assumed as a constant, at time « t ».

The powder layer, having infinitesimal thickness, must be in equilibrium under the action and the resulting reactions, due to friction, inter-particle inside the powder mass and on the side (die) walls.

The condition to fulfil is the following:

$$Ap = A(p - dp) + f\mu(p - dp/2)udx, \quad (1)$$

i.e.

$$Ap - A(p - dp) + Adp = f\mu pudx - f\mu \frac{dx}{2} udx. \quad (1')$$

Since it can be accepted that it is $dp \cdot dx \ll dp$ and $dp \cdot dx \ll dx$, and considering that, when the x -coordinate increases the pressure p decreases, by means of a series of simple mathematical passages the solu-

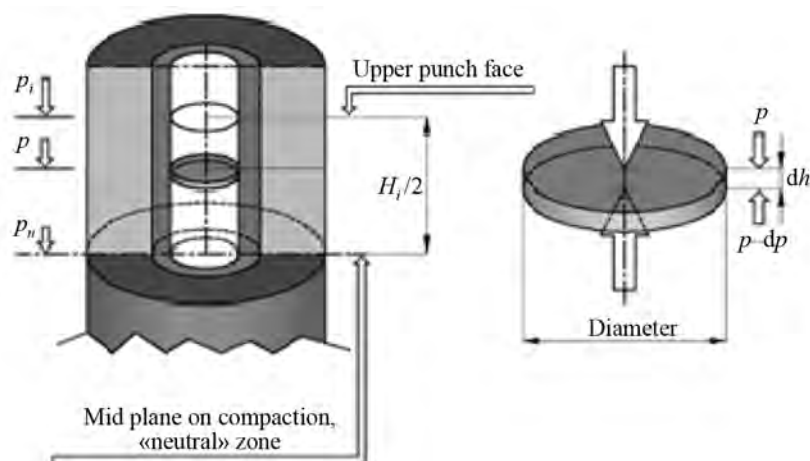


Fig. 8. Equilibrium conditions of a thin powder layer in presence of side wall friction

tion of relation (1) can be obtained and expressed as follows

$$p_n = p_0 \exp\left(-f\mu \frac{uH}{2A}\right), \quad (2)$$

where p_0 is the pressure exerted by the upper (or lower) punch.

Equation (2) indicates that the decrement of axial pressure is an increasing function of the friction coefficient. Plotting on a diagram, on a logarithmic scale, the p_n/p_0 ratio, as a function of the aspect ratio H/D (D being the diameter of a small cylinder, without holes) straight lines can be obtained.

The slope of these straight lines increases as the friction coefficient increases. It should be obvious that the decrement of axial pressure is much higher in the case of thin-walled hollow compacts.

Coming back to formula (2), being stated in advance that the axial pressure is constant on any horizontal section and on the face of the nearest acting punch, the law of variation given by the formula is valid only for high values of the ratio between friction area and compaction area. Such limitation can be easily accepted if the part geometry is characterized by a high ratio between side walls and compaction area. This condition is typical of many compact shapes, which may require quite high pressures to reach a given density. These increments of pressures, compared to the values typical of compressibility curves, come from the great extent of the area of side surfaces. Formula (2) enables evaluating the effects of friction on the axial pressure distribution. To go further, namely to evaluate the effects of pressure distribution on the average density, we should introduce a correspondence law between pressure and density. To be simple, we can consider the following semi-empirical relationship, going back to W.D. Jones, [30], and successfully applied by G.F. Bocchini, [31, 32]:

$$\gamma = a - bp + c\sqrt{p}, \quad (3)$$

where a , b and c are typical parameters of a given powder mix, which can be obtained from three couples of associated values of pressure and density. Within the test range, the densities that can be obtained at various pressures can be foreseen with a good enough approximation. However, any extrapolation requires caution. In fact, it may happen that extrapolating (3) beyond determinate pressures — not so far from the extremes of the range — indications physically unacceptable are drawn. At this stage, we can assume that previous hypothesis and equa-

tion (3), successfully applied to finite thicknesses, also holds for very thin powder layers. In this way, it is possible to find the analytical relationship, which relates average density with compact geometry, ratio between pressures, μ , and friction coefficient f . Remembering the above-mentioned hypotheses, if x is the distance between the surface under consideration and the nearest punch face, the average density, γ_m must be given by the integral function:

$$\gamma_m = \frac{2}{H} \int_0^{H/2} \gamma_x dx = \frac{1}{L} \int_0^L \gamma_x dx. \quad (4)$$

(For ease of writing and considering symmetric and bilateral compaction, it is better to refer to $L = H/2$). By inserting expression (4) into (3) we get

$$\gamma_m = \left[\frac{1}{L} \int_0^L a dx - \int_0^L b p dx + \int_0^L c \sqrt{p} dx \right], \quad (5)$$

i.e.

$$\gamma_m = \frac{a}{L} \int_0^L dx - \frac{b}{L} \int_0^L p dx + \frac{c}{L} \int_0^L \sqrt{p} dx. \quad (5')$$

According to (2), at a generic ordinate x it is

$$p = p_x = p_0 \exp(-f\mu ux/A) \quad (2')$$

so that equation (5') may be put in the form

$$\gamma_m = a - \frac{bp_0}{L} \int_0^L \exp\left(-f\mu \frac{ux}{A}\right) dx + \frac{c\sqrt{p_0}}{L} \int_0^L \exp\left(-f\mu \frac{ux}{2A}\right) dx. \quad (6)$$

From the solution of (6) by integration we get

$$\gamma_m = a + \frac{bp_0}{L} \frac{A}{f\mu u} \left[\exp\left(-f\mu \frac{ux}{A}\right) \right]_0^L - \frac{c\sqrt{p_0}}{L} \frac{2A}{f\mu u} \left[\exp\left(-f\mu \frac{ux}{2A}\right) \right]_0^L, \quad (7)$$

i. e.

$$\gamma_m = a + \frac{bp_0}{L} \frac{A}{f\mu u} \left[\exp\left(-f\mu \frac{uL}{A}\right) - 1 \right] - \frac{c\sqrt{p_0}}{L} \frac{2A}{f\mu u} \left[\exp\left(-f\mu \frac{uL}{2A}\right) - 1 \right]. \quad (8)$$

At first, formula (8) seems rather complicated. However, it can easily be expressed in a relatively simple form by gathering a few quantities, which are either in the fractions or as exponents, as follows:

$$\gamma_m = a + \frac{bp_0}{K_1K_2} [\exp(-K_1K_2) - 1] - \frac{2c\sqrt{p_0}}{K_1K_2} \left[\exp\left(-\frac{K_1K_2}{2}\right) - 1 \right]. \quad (9)$$

K_1 and K_2 are two dimensionless parameters, defined, respectively, by the following equations:

$$K_1 = f\mu, \quad K_2 = Hu/(2A), \quad (10)$$

where the previously explained quantities appear.

K_1 is a parameter of physical nature while K_2 is a geometrical one.

Expression (9) describes the relationship between the average density, the axial pressure exerted by punches, the ratio between the radial and the axial pressure, the wall friction coefficient and the geometry of any compact. For its practical use, in the strictest sense, the small test probes should have the same extent of lateral friction surface and, therefore, the same height. Consequently, the usual compressibility curves, obtained from samples having a constant weight, can be used only as an approximation. The previous formulas allow us to get, by calculation, sheaves of compressibility curves only if the same distribution of pressures assumed in the model proposed by A. Duffield and P. Grootenhuis, [29], can be applied to all the possible part shapes. Each curve of the sheaf characterizes a certain geometry of the parts, univocally defined by the dimensionless parameter K_2 . To make these calculations, the values of the friction coefficient and the values of the pressure ratio are needed. Useful data have been published by W.M. Long, [33], G. Bockstiegel and J. Hewing, [34], E. Ernst et alii, [35], and again E. Ernst, [36]. Both, f and μ , vary with pressure. Specifically, the friction coefficient decreases if pressure increases, according to a non-linear law, while the ratio between radial and axial pressures increases, fol-

lowing a nearly linear law. The results of compressibility test made on a high compressible iron powder, bulk-lubricated with 0.6 % Zn stearate, may be useful. Fig. 9 shows the experimental data and the calculated curve, by means of equation (3), at 400, 600 and 800 MPa. The equation of the curve is

$$\gamma = 2,763 - 0,00479p_0 + 0,29765\sqrt{p_0}.$$

Table 3 lists the physical and geometrical properties of the specimens pressed to plot the compressibility curve.

Fig. 10 shows the curves obtained using the relationship (10) to plot the compaction density of a same powder mix, at different pressures, versus the K_2 ratio between surfaces. Finally, Fig. 11 shows the curves of density for different values of K_2 . The upper curve is higher than that of compressibility measured according to the standard test conditions. As we can see, the compact geometry

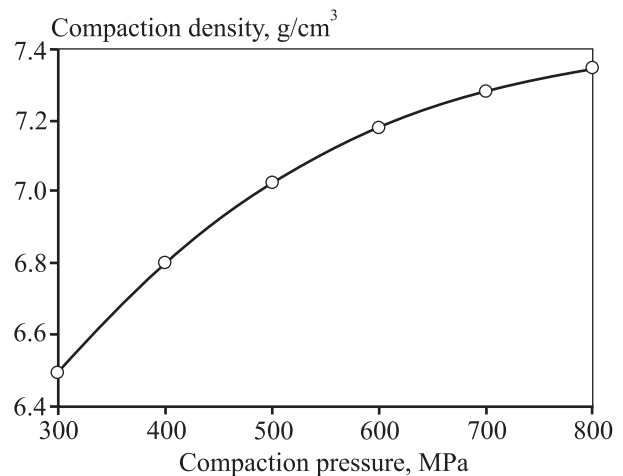


Fig. 9. Results of compressibility test (high compressibility atomized iron, bulk-lubricated) and curve calculated by means of equation (3)

Table 3. Physical and geometrical properties of the small cylindrical compacts utilized to plot the compressibility curve of a high compressible iron powder, bulk-lubricated (0.6 % Zn stearate)

Pressure, MPa	Density, g/cm³	Volume, cm³	Springback, %	Diameter, mm	Area A, mm²	Height, mm	Area S, mm²	K_2 ratio
300	6.500	10.769	0.09	25.023	491.76	21.90	1721.53	1.75
400	6.800	10.294	0.12	25.030	492.05	20.92	1645.08	1.67
500	7.030	9.957	0.15	25.038	492.35	20.22	1590.79	1.62
600	7.180	9.749	0.18	25.045	492.64	19.79	1557.09	1.58
700	7.285	9.609	0.21	25.053	492.94	19.49	1534.18	1.56
800	7.340	9.537	0.24	25.060	493.23	19.34	1522.23	1.54

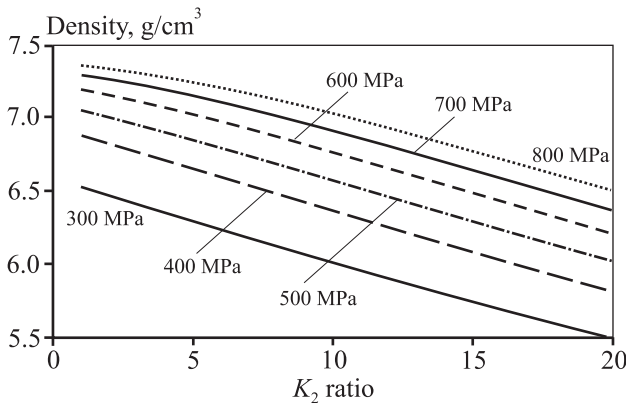


Fig. 10. Influence of K_2 ratio on compaction density; high compressibility iron powder, bulk lubricated (0.6 % zinc stearate)

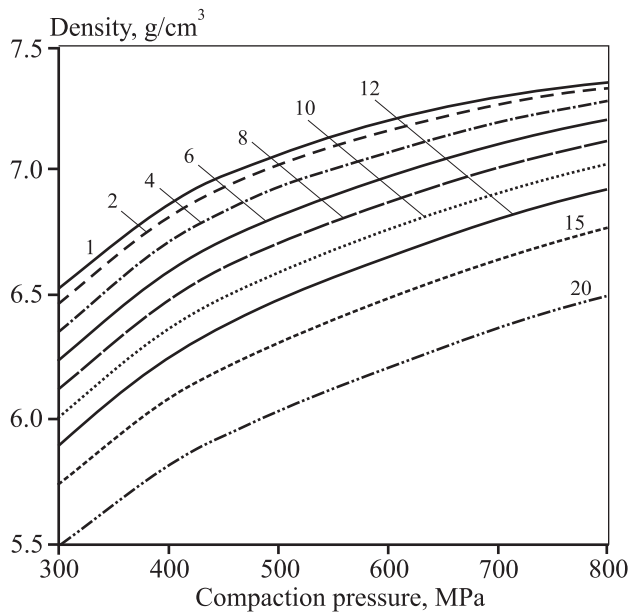


Fig. 11. Curves of compaction density for different values of K_2 ratio; high compressibility iron powder, bulk lubricated (0.6 % zinc stearate)

may have a significant impact on the pressures required to reach a certain density. To relationships used to plot the various curves are:

$$b^* = b \frac{K_1 K_2}{e^{-K_1 K_2} - 1}, \quad c^* = \frac{c}{2} \frac{K_1 K_2}{e^{-\frac{K_1 K_2}{2}} - 1},$$

$$\mu = 0,0005 p_a + 0,3219, \quad f\mu = 0,1.$$

The relationship between radial pressure and axial pressure is based on the experimental results of G. Böckstiegel and J. Hewing [34] and E. Ernst [35, 36], later confirmed by other scientists. In all experimental re-

search on powder compaction, it has been found that the friction coefficient between densifying powder and tool surfaces, for mass lubricated mixes, decreases when the applied pressure increases, [35, 36].

Friction on punch face with circular cross-section

Repeated experiences have shown that in case of compaction of a cylinder of height much larger than the average size of powder particles, (indicatively > 1000 times), the distribution of axial pressure is characterized by maximum values at the periphery and by one central area at nearly constant pressure, as schematically shown in Fig. 12. The different «motility» (the medical term «motility» appears apt to describe the possibility of displacement) of particles constrained near confining tool surfaces can explain the observed pattern of axial pressure distribution. In other words, the «degree of freedom» of particles far away from the compact «core» is reduced by the obstacles represented by die and punch surfaces. Differently, the powder granules at enough high distance from the confinement walls, especially vertical, are prevented from moving from their neighbor, equally stiff and resistant to plastic deformation. In these conditions, the resistance, which opposes displacements, is smaller, with consequent reduction of axial pressure on the punch that compresses the powder. Obviously, such a distribution of axial pressures appears also within the wall thickness of hollow shapes, if the horizontal and vertical dimensions are higher enough, in comparison to powder particles. The pressure distribution substantially changes when the part thickness is modest in compac-

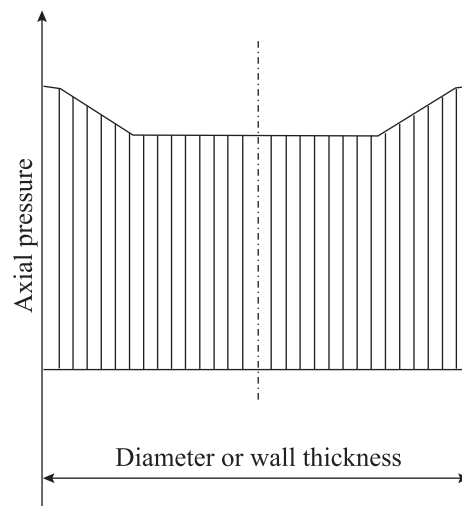


Fig. 12. Distribution of axial pressure for big enough compact size

tion direction. With similar geometries, the possibility of displacement of particles decreases, due to the «blocking» effect attributable to punch faces. To determine the distribution of axial pressure, when forming compacts of small height, we can consider the equilibrium conditions of an elementary powder volume on densification. For simplicity, let us suppose that the part shape is circular and that compaction is bilateral, simultaneous and symmetrical. Fig. 13 is the model used to find the relationships for effects, [37].

With reference to Fig. 13, H is the thickness of the compact. The equilibrium condition of an ideally isolated small quoin of powdered material, [33], is

$$\sigma_r H r d\theta + 2\sigma_\theta H d r \frac{d\theta}{2} = 2 f p r d\theta d r + (\sigma_r + d\sigma_r) H (r + d r) d\theta, \quad (11)$$

where f is the friction coefficient between punch faces and powder.

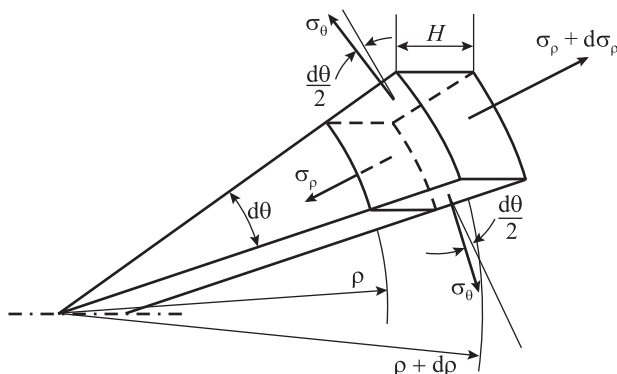


Fig. 13. Stresses acting on a small elemental sector (H thickness) during powder compaction

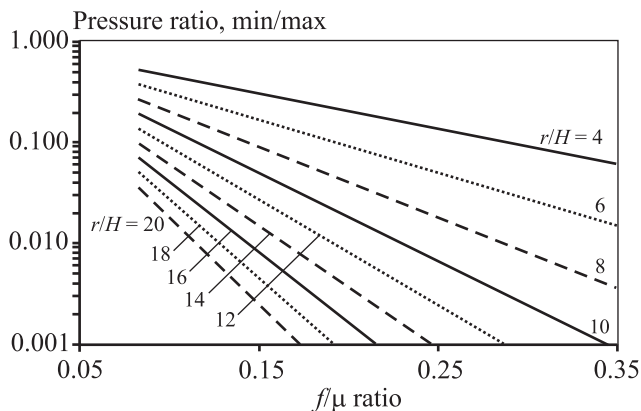


Fig. 14. Ratios between minimum axial pressure (on the outer radius) and maximum axial pressure (at the disk center), according to equation (18)

Both dr and $d\theta$ are sufficiently small, so as to neglect any variation of pressure, in the corresponding directions, on the horizontal faces of the small volume element. Therefore, we can assume that $\sin d\theta = d\theta$. If we divide equation (11) for $d\theta$ we get

$$\sigma_r H r + \sigma_\theta H d r = 2 f p r d r + H (\sigma_r r + \sigma_r d r + r d \sigma_r + d r d \sigma_r), \quad (12)$$

which, dividing by r and H and changing the sign, can be rearranged in the form

$$d\sigma_r + \frac{\sigma_r - \sigma_\theta}{2} d r = - \frac{2 f p}{H} d r \quad (13)$$

namely

$$\frac{d\sigma_r}{d r} + \frac{\sigma_r - \sigma_\theta}{r} = - \frac{2 f p}{H} \quad (13')$$

For reasons of isotropy in the directions orthogonal to the action of the applied pressure, it may be assumed that, on any horizontal plane, it is $\sigma_r = \sigma_\theta$. With this assumption, equation (13') becomes

$$\frac{d\sigma_r}{d r} = - \frac{2 f p}{H}, \quad (14)$$

where: σ_r is the stress acting in radial or tangential direction, p is the pressure acting in axial sense; its value depends on the considered point, i.e. on the position along a radius.

It can be now useful to repeat, as stated in [37], a short digression on the apparent contradiction between the dimensions of the elemental sector: two of them, dr and $d\theta$, are infinitesimal, whilst the height H is finite. Furthermore, the considered geometry seems to contradict, at least at first glance, what has been developed by A. Duffield et alii, [29], where the pressure variation in axial direction, between two horizontal planes placed at a short distance, dh , each other, has been expressly considered. Actually, for whichever horizontal plane inside the hardening powder mass, at a sufficiently high distance from the punch faces, the distribution of the axial pressures can be approximated by a constant course. On the contrary, the friction between punch faces and powder univocally determines the axial pressure distribution. The law of variation in radial sense depends on several factors, among which the distance from the extremity horizontal faces certainly prevails. In the case of high axial thicknesses, clearly, the assumption of a constant radial pressure is unacceptable and, more correctly, it should be replaced by an integral function. Conversely, in the case of relatively modest heights, the variation of radial pressures in vertical direction can be

considered negligible. Therefore, the equilibrium condition expressed by (11) can be allowed, provided that the H height is small enough. A proportionality relationship, [33–36], links radial and axial pressure (having the latter a specific value):

$$p_r = \mu p_a \text{ (with } \mu = \mu(p_a) < 1 \text{ and } \mu = \mu(p_a)). \quad (15)$$

Therefore, remembering also the equality between stresses and local pressures, formula (14) may be modified as follows:

$$\frac{dp_r}{dr} = -\frac{2fp_a}{H} \quad (16)$$

and again, simply indicating with p the axial pressure acting on the small element of the area,

$$\mu \frac{dp}{dr} = -\frac{2fp}{H} \quad (16')$$

namely

$$\frac{dp}{p} = -\frac{2fdr}{\mu H}. \quad (16'')$$

The indefinite integral of equation (16'') is

$$\ln p = -\frac{2f}{\mu} \frac{r}{H}, \quad (17)$$

which, transforming the logarithm in a power expression, gives

$$p = p_0 \exp\left(-\frac{2f}{\mu} \frac{r}{H}\right), \quad (18)$$

where p is the axial pressure which acts on the powder at a distance r from the center of the figure, p_0 is the axial pressure acting on the center of the compaction area, that is for $r = 0$.

If we now introduce two dimensionless parameters, one of physical in nature, $M_1 = 2f/\mu$, and one of geometrical nature, $M_2 = r/H$, the equation (18) can be written as

$$p = p_0 \exp(-M_1 M_2). \quad (18')$$

The equations (17) and (18) indicate that the axial pressure on the faces of the powder mass on densification decreases along the radius, following a logarithmic law. The maximum value appears at the center, whereas the minimum value occurs on the circumference. The gradient of pressure, in radial direction, depends on:

- friction coefficient between punch faces and powder on densification;
- ratio between radial and axial pressure;
- geometry of the part.

It may be useful to remark that the dimensionless pa-

rameter M_1 is formally the inverse of the dimensionless parameter K_1 found in the analytical evaluation of the effect of friction between powder mix on densification and confining die walls. However, we should consider that the lubrication conditions and possibilities of movement of powder particles, in the two cases, are substantially different.

The geometric parameter, M_2 , is instead a ratio between two lengths. M_2 also turns out to be the inverse of K_2 parameter, previously found. Eq. (18) enabled to plot the graph of Fig. 14. The two quantities f and μ vary, with different laws, as functions of the compaction pressure. The stronger variation regards the friction coefficient, for bulk-lubricated powders mass: it can decrease from 0.2 to less than 0.05 as p increases, while, in the same range, m increases from about 0.5 to almost 0.7, [34, 36, 37]. Any effort to identify limitations and inaccuracies arising from the assumptions here made would require some specific investigation, on disks with different thin thickness and under different lubrication conditions of the punch faces. In addition, to take account of any change of friction coefficient, the experimental verifications should be repeated at different pressures. Independently of any targeted experimental investigation, it is notoriously difficult to comply with flatness tolerances on the faces of thin disks, which systematically tend to bulge at the center (few hundredths of a millimeter). The observed bulges replicate the different local elastic yielding of punches, coming from difference among local stress levels. By way of example, in the case of a 32 mm diameter and 2 mm height disk, the r/H ratio is 8.0. Assuming an average value of the f/μ ratio, according to the graph of Fig. 14, the axial pressure acting on the outermost zone is equal to nearly 30 % of that acting on the center, to drop to less than 1 % if r/H becomes equal to 20.

Axial pressure distribution in the case of circular shapes

If F indicates the force applied on compaction by the upper (and lower) punch, the average axial pressure, p_m , acting on a small disk with a radius at compaction end is

$$p_m = \frac{F}{\pi a^2}. \quad (19)$$

More, if we consider that the axial pressure varies along a radius, it should be

$$F = p_m \pi a^2 = \int_0^a 2p \pi r dr \quad (20)$$

and also

$$p\pi a = 2\pi \int pr dr. \quad (21)$$

If we insert in Eq. (21) the expression of local pressure given by Eq. (18) and divide by π , we get

$$p_m a^2 = 2p_0 \int_0^a r \exp(-M_1 M_2) dr \quad (22)$$

that, remembering the definition of M_2 , becomes

$$p_m = \frac{2p_0}{a^2} \int_0^a r \exp\left(-\frac{M_1}{H} r\right) r dr. \quad (22')$$

Only for formal simplicity, let us write

$$b = M_1/H. \quad (23)$$

Then, from (22), we have

$$p_m = \frac{2p_0}{a^2} \int_0^a r \exp(-br) dr \quad (24)$$

and also

$$\frac{p_m a^2}{2p_0} = \int_0^a r \exp(-br) dr. \quad (25)$$

The integral of the second term of (25) may be solved as follows

$$\int_0^a r \exp(-br) dr = \left[\frac{-\exp(-br)}{b^2} (br + 1) \right]_0^a \quad (26)$$

namely

$$\begin{aligned} \int_0^a r \exp(-br) dr &= \frac{1}{b^2} [(-\exp(-br))(br + 1)]_0^a = \\ &= \frac{1}{b^2} [1 - (\exp(-ba))(ba + 1)]. \end{aligned} \quad (26')$$

If we insert the solution of the integral given by (26') in (25), remembering that it is $bH = M_1$ and indicating by M_{2max} the value corresponding to the outside radius of the disk, we get

$$p_0 = \frac{p_m (M_1)^2 (M_{2max})^2}{2[1 - (\exp(-M_1 M_{2max})) (M_1 M_{2max} + 1)]}. \quad (27)$$

This formula establishes the relationship between average and maximum pressure, which acts on the center of the disk. By analogy with the indications given by formula (19), at equal average pressure, the maximum value depends on compact geometry and friction coefficient.

It may be interesting to try to see graphically how the maximum pressure at the center of the disk varies as a function of M_1 and M_2 values. The trends are plotted

in Fig. 15, which shows that the maximum calculated pressure at the center of the disk strongly increases as the thickness/radius ratio decreases.

The influence of the M_1 ratio ($M_1 = 2f/\mu$) is remarkable: at the same M_{2max} , ($M_{2max} = a/H$, a being the outer radius of the «thin» disk), the value of the maximum pressure at the center could theoretically increase, to become 4 or 5 times greater than the average one. It should also be noted that M_1 values lower than 0.4 have been considered, remembering that friction coefficient decreases at increasing pressure on bulk-lubricated powder.

Obviously, the curves of Fig. 15 cannot describe real situations, since it should be assumed that the most heavily loaded areas of the punches deforms elastically and tend to involve the adjacent ones, less stressed, with a tendency towards reduction of the differences between local stresses.

The lenticular-type deformations usually observed on thin plates or disks, as already mentioned, appears as

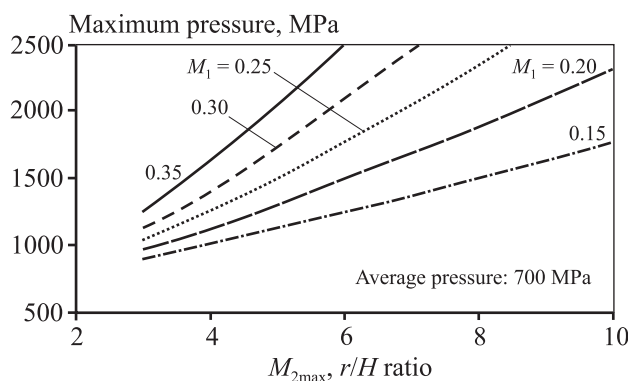


Fig. 15. Variation of the maximum pressure, at the center of a thin disk, as a function of the ratio between radius and height (or thickness)

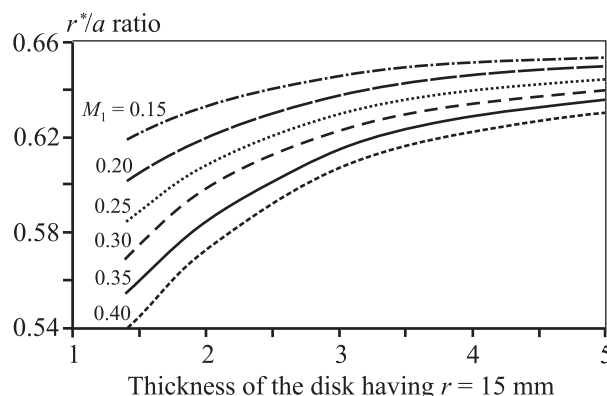


Fig. 16. Position of r^* radius, ($r^* = r/a$), where the axial pressure is equal to the average one, function of the thickness of a «thin» disk having a radius

an indirect confirmation of this hypothesis. For a specific radius r^* , ($0 < r^* < a$), the axial pressure should have (on a specific radius) the same value of the average one, given by (22). According to (19), (21) and (22), when it is $r = r^*$, it should also be:

$$p_{r^*} = p_0 \exp(-M_1 r^*/H) = p_m. \quad (28)$$

If we insert in Eq. (28) the expression of p_0 given by (27), after elimination of the exponential we get

$$\frac{r^*}{H} = \frac{1}{M_1} \ln \frac{(M_1)^2 (M_{2\max})^2}{2[1 - (\exp(-M_1 M_{2\max})) (M_1 M_{2\max} + 1)]}. \quad (29)$$

This formula defines the variation law of the position of r^* , due to changes of physical and geometrical quantities involved. As Fig. 16 shows, the r^* radius tends to approach the part center when friction coefficient increases and thickness of the disk decreases. The variation range, anyhow, is relatively modest: from 0.54 to 0.66. Only by way of example, let us suppose that the flatness defect observed on a 30 mm diameter disk is 0.05 mm. This deformation, on a 100 mm long punch, corresponds to a difference between axial stresses of the order of 100 MPa. This value allows to assume that, as a result of different local elastic yielding of the punches, the effective radius of the area in which the local pressure is greater than the average is significantly larger than r^* . As a first approximation, in absence of other indications, we imagine to split into two equivalent areas the annulus defined by the radii r^* and a , and suppose that the area subject to local axial pressure greater than or equal to the average one includes the circle of radius r^* and half of the outside area. On the basis of the bundle of curves of Fig. 17, we can admit that, for a 3 mm thick disk, on the average, it is $r^* = 0.62a$. In this

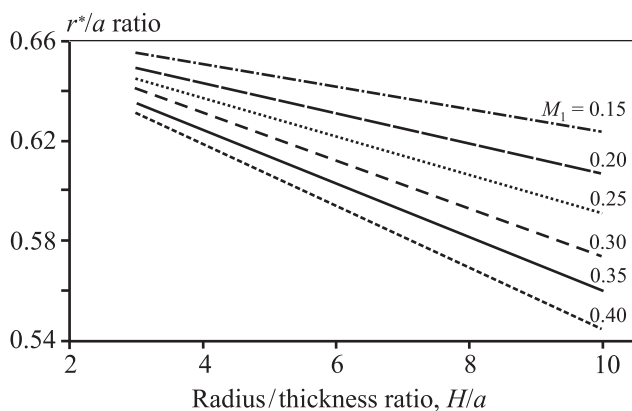


Fig. 17. Position of the radius on which the local axial pressure is equal to the average one, as a function of $M_{2\max}$ ratio

case, the formal expression of the assumptions made, for $r = 1.00$ mm, is

$$\pi \cdot 1 \cdot 0.62^2 + \frac{\pi(1^2 - 0.62^2)}{2} = 2.175 \text{ mm}^2. \quad (30)$$

This area corresponds to 69 % of the total surface. If we accept the proposed hypotheses, we can conclude that the «effective» pressure acts on an area that is approximately equal to 70 % of the total. Case by case, the curves of Fig. 16 allow obtaining less approximate indications.

As shown in Fig. 17, as the a/H ratio increases, i.e. as the relative thickness of the disc decreases, the r^* radius tends towards the center, with a linear law. In this way, also the area that we can consider «effective» for powder densification, i.e. the area where the local axial pressure is equal to or greater than the average one, decreases.

Decrease of average density of thin disks

Within the explored fields, (M_1 and $M_{2\max}$ variables), the ratio between the area that can be considered effective for densification and the total one varies between 0.65 and 0.71. Given the modest variation, we can assume that the «effective» compressibility curves move downward, in comparison to the standard ones, as Fig. 18 shows. In other words, this corresponds to admit that, in the case of thin plates or disks, the real behavior of the powder in densification is worse than the standard, as if the powder becomes less compressible.

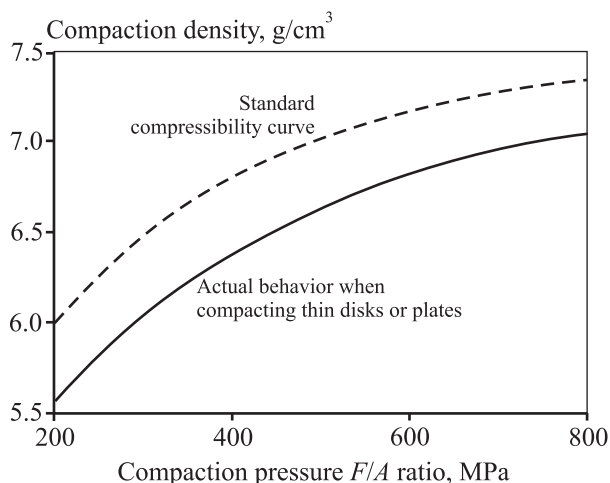


Fig. 18. Standard compressibility curve and «effective» compressibility curve for compacting low-thickness plates and disks

In Fig. 18, the compressibility curve that we can define «effective» is unique, but, in reality, given the effects of M_1 and M_2 , we can imagine the existence of a bundle of «actual» compressibility curves, spaced apart in dependence of friction coefficient and thickness/radius ratio. Another reason for the decrease of the average density of thin disks (or plates) derives from the presence of two «boundary layers», within which the density increases gradually proceeding towards the interior. These boundary layers, generated by reduced motility of particles directly in contact with the punch faces, have thicknesses depending on average particle size of the used powder, as found by G.F. Bocchini, [38]. Their effect on the average density is greater as the thickness of disk decreases. The presence of a boundary layer less dense than the average for the particular involves a whole series of possible consequences on the mechanical behavior in operation of sintered parts. The analysis of this aspect, however, is beyond the scope of this work.

Support of experimental data

This theoretical study is not corroborated by any joint experimental investigation on density variations of compacts (and/or sintered parts) attributable to typical geometries and influenced by negative effects of friction resistance at tool walls. In the literature, however, there are some indications that agree with the assumptions and analytical developments here outlined. Fig. 19, for instance, shows a graph based on the data published

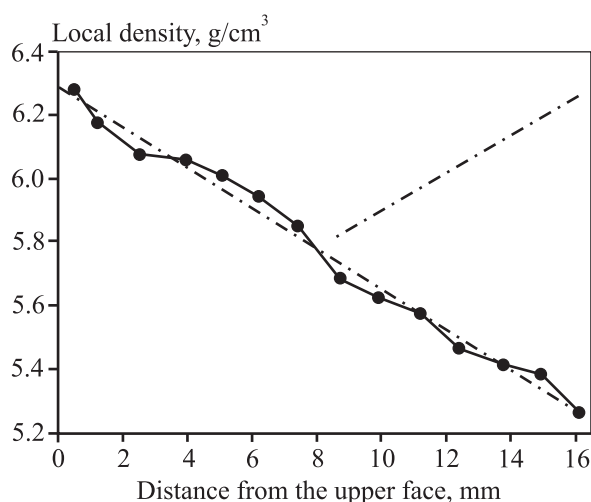


Fig. 19. Density distribution, in axial sense, of a iron bushing 16 mm high, uniaxially compacted. On the right, ideal line, corresponding to bilateral compaction, with $K_2 = 16$ (from G. Mair [39], redrawn)

by G. Mair, [39], who measured, by slices, the density distribution of cylindrical bushings (16 mm nominal height), obtained by unilateral compaction of a high compressibility iron powder, bulk-lubricated with 1 % micronized wax. On the same figure there is the ideal line corresponding to a correct (symmetrical) compaction. On the figure, each dot indicates the density of a small height ring, cut at a given mean distance from the end face formed by the punch. As we can observe, the density decrease in axial direction shows a linear trend. In the same work, Mair presents other graphs, relating to bushes of different geometry, which confirm the dependence of the local density and — consequently — also on the average one, from the geometric parameter K_2 . Furthermore, in the case of very high compaction pressure (between 810 and 920 MPa), other conditions being equal, the gradients of the curves of local density decrease, as the pressure increases, for a sort of «saturation» effect. In other words, at very high density the effect of pressure increases on density variations progressively decreases. The reason is that the more dense zones have very limited possibility, if any, of further densification. For most metals, any compressibility curve shows some trend to flatten as pressure increases.

G.F. Bocchini et alii, [40, 41], published a series of experimental results, obtained in a study made to confirm — or reject — the conclusions of a theoretical study on friction effects during compaction, [37]. The research investigated the possible density decreases of thin compacts vs. their thickness, on small discs as specimens ($\Phi = 25$ mm, high or normal compressibility iron powder), with different lubricants and lubrication type. The green disks were presintered, to remove lubricants and to get a mechanical strength of samples compatible with the preparation of metallographic specimens, for stratigraphic observation and assessment of porosity gradients. The average density was measured by Archimedes' method. Fig. 20 and 21 show the density distribution of presintered disks, for 5 different lubrication conditions. On each case, the curves seem reach a horizontal trend as K_2 is > 0.5 . It is also interesting to observe the effect of wall lubrication, with a remarkable density increase in the range $0.1 < K_2 \leq 0.4$. In the same investigation, G.F. Bocchini et alii, [40, 41], measured, by image analysis, the porosity variations vs. the distance from the face formed by a punch. Fig. 22 shows the results of those evaluations for disks obtained from atomized iron powder. The results obtained on samples based on sponge powder were similar. In both cases, within a very thin layer, proceeding from the outer surface towards the

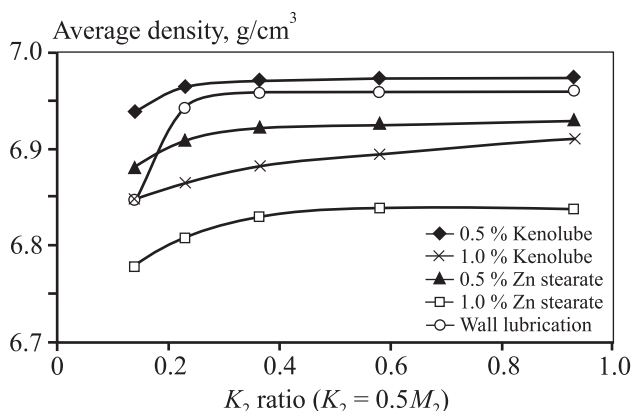


Fig. 20. Average density of presintered thin disks versus the geometrical parameter K_2 . Sponge powder (NC 100.24, from Höganäs AB); Compaction pressure 600 MPa (from [41, 42])

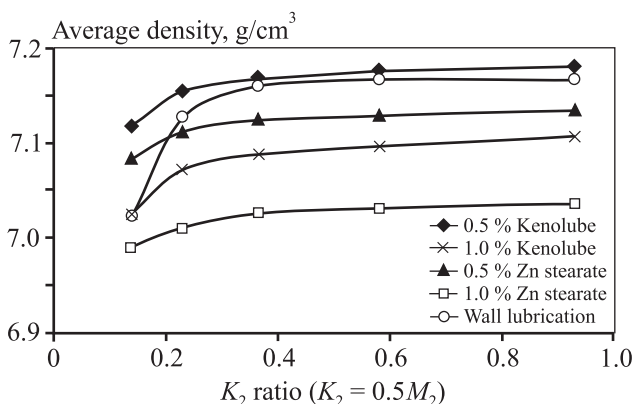


Fig. 21. Average density of presintered thin disks versus the geometrical parameter K_2 . Atom. powder (ASC 100.29, from Höganäs AB); Compaction pressure 600 MPa (from [41, 42])

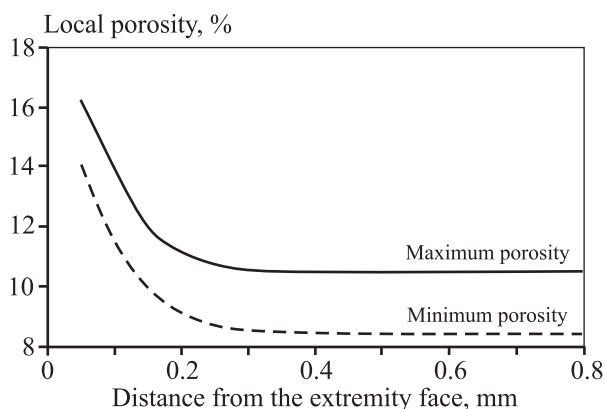


Fig. 22. Trend of porosity, inside thin surface layers, of presintered thin disks. Atomized iron powder, bulk-lubricated or with wall lubrication (from G.F. Bocchini et alii [40, 41])

part interior, the porosity decreases. As we can see, the boundary layer extends inward to about 0.3 mm. We should remember that the average size of a typical granule of atomized iron powder is about 0.1 mm. This trend, which any careful check on green or sintered parts can easily confirm, seems support the hypothesis of boundary layers formed on compaction and attributable to reduced local «motility» of powder particles, constrained by punch faces.

Conclusions

The pressure distributions during metal powder compacting, on die and punch faces, have been determined by simple geometrical models. The pressure drop increases as friction coefficient between powder mixes and tool surfaces increases. Uneven pressure distributions cause a decrease of average compact density, in comparison with the values drawn from standard compressibility curves.

In fact, since density increases, as compaction pressure increases, according to a non-linear law, if the axial pressure is uneven, the corresponding average density will be lower than that ideally obtained in case of constant pressure.

The analytical study on density decrease of compacts having relatively small thickness has allowed the formulation of equations relating average density and geometry. Two dimensionless parameters, K_2 and M_2 , which depend on the areas of compaction surface and side surfaces (die confining surface, and punch surfaces acting as die) affect pressure and density distributions. In case of part shapes strongly different from the standard specimens, the gap between indications given by usual curves and actual powder behavior may reach dangerous levels. The actual pressure differences may be so high as to imperil the integrity of some tool items or even press components. If the compact shapes are similar to thin disks or plates, a further decrement of the average density occurs, in comparison with standard curves, which depends on the presence of boundary layers with varying density. These boundary layers are always present, but their relative weight increases as part thickness decreases. More, if the parts have a small axial thickness and a relatively large compaction area, the axial pressure gradients may lead to flatness defect. According to the theoretical approach, such parts should always present a lenticular shape, with thickness difference increasing as thickness decreases. This result seems to explain some quality problems regarding flatness tolerance of thin parts.

Since the standard compressibility curves appear unsuitable to assess the compaction behavior of metal powders for different shapes, calculation methods suitable to plot approximate compressibility curves are presented. In conclusion, the answer to the dilemma of the title may be only one: the standard curves are useful to compare different powders, but are definitely unsuitable — or even dangerous — for any reliable forecast of stress levels actually acting on various elements of compaction tools.

References

1. *Squire A.* Density relationship of iron powder compacts. *Trans AIME*. 1947. Vol. 171. P. 485.
2. *Lee P.W.* Pressed and sintered parts and their applications. In: *Powder metallurgy, applications, advantages and limitations*. Chapter 4. Ed. E. Klar. Ohio: ASM, Metals Park, 1983.
3. *Lenel F.V.* Powder metallurgy. Principles and applications. Princeton, New Jersey: Metal Powders Industries Federation (MPIF), 1980.
4. *Kosko J.* Mechanical properties of high-performance powder metallurgy parts. In: *ASM Metals Handbook. Vol. 7. Powder metals technologies and applications*. Ohio: ASM, Metals Park, 1998.
5. *Kieffer R., Hotop W.* Sintereisen und sinterstahl. Wien: Springer Verlag, 1948.
6. *Balshin M.Ju.* *Dokl. Akad. Nauk SSSR*. 1949. Vol. 67. P. 831—837.
7. *Balshin M.Ju.* Pulvermetallurgie. Halle (Saale): Veb Wilhelm Knapp Verlag, 1954.
8. *Knopp W.V.* Sintered nickel steels — the path to improved properties. In: *Progress in powder metallurgy: 6th Annual Meeting of MPIF*. Chicago, 1960.
9. *Pisarenko G.S., Troshchenko V.T., Krasovskii A.Ya.* Study of the mechanical properties of porous iron in tension and torsion. In: *Iron powder metallurgy*. N.Y.: Plenum Press, 1968. P. ?
10. *Hausner H.H.* Handbook of powder metallurgy. N.Y.: Chemical Publishing Co. Inc., 1973.
11. Ferrous powder metallurgy materials: ASM Metals Handbook. 9 ed. Vol. 1. Ohio: American Society for Metals, Metals Park, 1978.
12. *German R.M.* Porous materials. In: *Advances in powder technology: ASM Materials Science Seminar* (Louisville, 1981). Ed. G.Y. Chin. Ohio: ASM, Metals Park, 1982.
13. *DeHoff R.T., Gillard J.P.* Modern developments in powder metallurgy. Vol. 4. Ed. H.H. Hausner. N.Y.: Plenum Press, 1971.
14. *German R.M.* Powder metallurgy science. Princeton, New Jersey: MPIF, 1994.
15. *Thümmler F., Oberacker R.* Introduction to powder metallurgy. Eds I. Jenkins, J.V. Wood. London: The Institute of Materials Science on Powder Metallurgy, 1993.
16. *Zapf G.* Handbuch der Fertigungstechnik. Bd. 1. Urformen. Kap. 4. Hrsg. G. Spur. München: Hanser-Verlag, 1981.
17. *Schatt W., Wieters K.P.* Powder metallurgy, processing and materials. Shrewsbury, UK: European Powder Metallurgy Association (EPMA), 1997.
18. *Beiss P., Börnstein L.* Group VIII: Advanced materials and technologies. Vol. 2. Materials, Subvol. A: Powder metallurgy data, Pt. 1. Metals and magnets. Berlin Heidelberg, N.Y.: Springer-Verlag, 2003.
19. *Beiss P.* Pulvermetallurgische Fertigungstechnik. Berlin-Heidelberg, N.Y.: Springer-Verlag, 2013.
20. Standard 35: Materials standards for PM structural parts. Princeton, New Jersey: Metal Powder Industries Federation (MPIF), 2009.
21. Iron and steel powders for sintered components. Sweden: Höganäs AB, 2002.
22. *Eudier M.* Propriétés mécaniques des aciers frittés. *Planseeberichte für Pulvermetallurgie*. 1966. Vol. 14 (29).
23. *Bocchini G.F.* The influences of porosity on the characteristics of sintered materials. SAE Int. Congress and Exposition (Detroit, Michigan, 24—28 Febr., 1986). SAE Technical Paper 860148.
24. *Exner H.E., Pohl D.* Fracture behavior of sintered iron. *Powder Metall. Int.* 1978. Vol. 10 (4). P. 193.
25. Standard test method for compressibility of metal powders in uniaxial compaction: ASTM B331-85. Philadelphia, USA: American Society for Testing and Materials (ASTM), Nov. 1985.
26. Method for determination of compactibility (Compressibility) of «Metal Powders»: MPIF Standard 45. Princeton, New Jersey, USA: Metal Powder Industries Federation (MPIF), 1988.
27. Metallic powders, excluding powders for hard metals — Determination of compactibility (compressibility) in uniaxial compression: ISO Standard 3927. International Standard Organization (ISO), 1977.
28. *James W.B.* Microstructure development. EPMA PM Summer School (Acqui Terme, Italy, 22—29 June, 2008).
29. *Duffield A., Grootenhuis P.* Pressing characteristics of air-atomized copper powders: Special Report No. 58. In: *Symposium on Powder Metallurgy*. London: The Iron and Steel Institute, 1956.
30. *Jones W.D.* Fundamental principles of powder metallurgy. London: Edward Arnold (Ltd.) Publ., 1960.
31. *Bocchini G.F.* Density reduction due to wall friction

- during compaction — A theoretical approach for a reliable quantitative evaluation. In: *Horizons of powder metallurgy*. Part II: Int. Powder Metallurgy Conference and Exhibition «P/M 1986» (Düsseldorf, 7—11 July, 1986). Verlag Schmid, Freiburg, 1986. P. 849—852.
32. Bocchini G.F. Diminuzioni di densità nella pressatura dei pezzi in metallurgia delle polveri, causate dagli attriti alle pareti — Un approccio teorico per una valutazione quantitativa affidabile. In: *5 Convegno Nazionale su «Tribologia, attrito, usura e lubrificazione»*, AIM e ASMECCANICA (Sorrento, Italy, 7—9 Oct., 1987); *La metallurgia italiana*. 1989. Vol. 81. No. 7—8. P. 613—621.
 33. Long W.M. Radial pressures in powder compaction. *Powder Metall.* 1960. No. 6. P. 73—86.
 34. Bockstiegel G., Hewing J. Verformungsarbeit, Verfestigung und Seitendruck beim Pressen von Metallpulvern. In: *3rd Europ. Symp. on Powder Metallurgy* (Stuttgart, 1968). Chapt. 1.2, 32.
 35. Ernst E., Thümmel F., Beiss P., Whäling R., Arnhold V. Friction measurements during powder compaction. *Powder Metall. Intern.* 1991. Vol. 23. No. 2. P. 77—84.
 36. Ernst E. Axiale Pressvorgänge in der Pulvermetallurgie. Fortschrittberichte VDI, Reihe 2: Fertigungstechnik. Nr. 259. Düsseldorf: VDI Verlag, 1992.
 37. Bocchini G.F. Friction effects in metal powder compaction. Part 1. Theoretical aspects. In: *Int. Conf. on P/M and particulate materials* (Seattle, 14—17 May, 1995).
 38. Bocchini G.F. Influence of small die width on filling and compacting densities. *Powder Metall.* 1987. Vol. 30. No. 4.
 39. Mair G. Correlation between axial density and friction in the compaction and ejection of PM shapes. In: *Metal Powder Report*. Elsevier Science Publ. Ltd., Sept. 1991. P. 60—64.
 40. Bocchini G.F., Fontanari V., Molinari A. Friction and boundary layer effects on the apparent compressibility of iron powders determined on thin disks. In: *P/M World Congress* (Paris, 6—9 June, 1994).
 41. Bocchini G.F., Fontanari V., Molinari A. Friction effects in metal powder compaction part two. Experimental results. In: *APMI/MPIF PM International Conf.* Seattle, WA, 1995.